

Fully Finite Element Adaptive AMG Method for Time-Space Caputo-Riesz Fractional Diffusion Equations

X. Q. Yue¹, W. P. Bu¹, S. Shu^{2,*}, M. H. Liu¹ and S. Wang¹

¹ School of Mathematics and Computational Science, Xiangtan University, Hunan 411105, China

² Hunan Key Laboratory for Computation and Simulation in Science and Engineering, Xiangtan University, Hunan 411105, China

Received 4 February 2018; Accepted (in revised version) 17 April 2018

Abstract. The paper aims to establish a fully discrete finite element (FE) scheme and provide cost-effective solutions for one-dimensional time-space Caputo-Riesz fractional diffusion equations on a bounded domain Ω . Firstly, we construct a fully discrete scheme of the linear FE method in both temporal and spatial directions, derive many characterizations on the coefficient matrix and numerically verify that the fully discrete FE approximation possesses the saturation error order under $L^2(\Omega)$ norm. Secondly, we theoretically prove the estimation $1 + \mathcal{O}(\tau^\alpha h^{-2\beta})$ on the condition number of the coefficient matrix, in which τ and h respectively denote time and space step sizes. Finally, on the grounds of the estimation and fast Fourier transform, we develop and analyze an adaptive algebraic multigrid (AMG) method with low algorithmic complexity, reveal a reference formula to measure the strength-of-connection tolerance which severely affect the robustness of AMG methods in handling fractional diffusion equations, and illustrate the well robustness and high efficiency of the proposed algorithm compared with the classical AMG, conjugate gradient and Jacobi iterative methods.

AMS subject classifications: 35R11, 65F10, 65F15, 65N55

Key words: Caputo-Riesz fractional diffusion equation, fully discrete space-time FE scheme, condition number estimation, algorithmic complexity, adaptive AMG method.

1 Introduction

In recent years, there has been an explosion of research interest in numerical solutions for fractional differential equations, mainly due to the following two aspects: (i) the huge

*Corresponding author.

Emails: yuexq@xtu.edu.cn (X. Q. Yue), weipingbu@xtu.edu.cn (W. P. Bu), shushi@xtu.edu.cn (S. Shu)

majority can't be solved analytically, (ii) the analytical solution (if luckily derived) always involves certain infinite series which sharply drives up the costs of its evaluation. Numerous numerical methods have been proposed to approximate more accurately and faster, such as finite difference (FD) method [1–11], finite element (FE) method [12–20], finite volume method [21] and spectral (element) method [22–27]. An essential challenge against standard differential equations lies in the presence of the fractional differential operator, which gives rise to nonlocality (space fractional, nearly dense or full coefficient matrix) or memory-requirement (time fractional, the entire time history of evaluations) issue, resulting in a vast computational cost.

Preconditioned Krylov subspace methods are regarded as one of potential solutions to the aforementioned challenge. Numerous preconditioners with various Krylov subspace methods have been constructed for one- and two-dimensional, linear and nonlinear space-fractional diffusion equations (SFDE) [28–31]. Multigrid method has been proven to be a superior solver and preconditioner for ill-conditioned Toeplitz systems as well as SFDE. Pang and Sun proposed an efficient and robust geometric multigrid (GMG) with fast Fourier transform (FFT) for one-dimensional SFDE by an implicit FD scheme [32]. Bu et al. employed this GMG to multi-term time-fractional advection-diffusion equations via a fully discrete scheme by FD method in temporal and FE method in spatial direction [33]. Jiang and Xu constructed optimal GMG for two-dimensional SFDE to get FE approximations [34]. Chen et al. made the first attempt to present an algebraic multigrid (AMG) method with line smoothers to the fractional Laplacian through localizing it into a nonuniform elliptic equation [35]. Zhao et al. invoked GMG for one-dimensional Riesz SFDE by an adaptive FE scheme using hierarchical matrices [36]. Chen and Deng exploited GMG's coarsening strategy and grid-transfer operators, equipped with Galerkin coarse-grid operator to produce a robust multigrid for nonlocal models in a finite range of interactions [37]. From the survey of references, despite quite a number of contributions to numerical methods and preconditioners, there are no calculations taking into account of fully discrete FE schemes and AMG methods for time-space Caputo-Riesz fractional diffusion equations.

In this paper, we are concerned with the following time-space Caputo-Riesz fractional diffusion equation (CR-FDE)

$${}_0^C D_t^\alpha u(x,t) = \frac{\partial^{2\beta} u(x,t)}{\partial |x|^{2\beta}} + f(x,t), \quad t \in I = (0, T], \quad x \in \Omega = (a, b), \quad (1.1a)$$

$$u(x,t) = 0, \quad t \in I, \quad x \in \partial\Omega, \quad (1.1b)$$

$$u(x,0) = \psi_0(x), \quad x \in \Omega, \quad (1.1c)$$

with orders $\alpha \in (0,1)$ and $\beta \in (1/2,1)$, the Caputo and Riesz fractional derivatives are respectively defined by

$${}_0^C D_t^\alpha u = \frac{1}{\Gamma(1-\alpha)} \int_0^t (t-s)^{-\alpha} \frac{\partial u}{\partial s} ds, \quad \frac{\partial^{2\beta} u}{\partial |x|^{2\beta}} = -\frac{1}{2\cos(\beta\pi)} ({}_x D_L^{2\beta} u + {}_x D_R^{2\beta} u),$$

where

$${}_x D_L^{2\beta} u = \frac{1}{\Gamma(2-2\beta)} \frac{\partial^2}{\partial x^2} \int_a^x (x-s)^{1-2\beta} u ds, \quad {}_x D_R^{2\beta} u = \frac{1}{\Gamma(2-2\beta)} \frac{\partial^2}{\partial x^2} \int_x^b (s-x)^{1-2\beta} u ds.$$

The remainder of this paper proceeds as follows. A fully discrete FE method of (1.1a)-(1.1c) is developed in Section 2. Section 3 comes up with the theoretical estimation and verification experiments on the condition number of the coefficient matrix. The classical AMG method is introduced in Section 4 followed by its uniform convergence analysis and the construction of an adaptive AMG method. Section 5 reports and analyzes numerical results to show the benefits. We close in Section 6 with some concluding remarks.

2 Fully discrete finite element scheme for the CR-FDE

For simplicity, following [38], we will use the symbols \lesssim, \gtrsim and \simeq throughout the paper. $u_1 \lesssim v_1$ means $u_1 \leq C_1 v_1$, $u_2 \gtrsim v_2$ means $u_2 \geq c_2 v_2$ while $u_3 \simeq v_3$ means $c_3 v_3 \leq u_3 \leq C_3 v_3$, where C_1, c_2, c_3 and C_3 are generic positive constants independent of variables, time and space step sizes.

2.1 Reminder about fractional calculus

In this subsection, we briefly introduce some fractional derivative spaces and several auxiliary results. Here the L^2 inner product and norm are denoted by

$$(u, v)_{L^2(\Omega)} = \int_{\Omega} u v dx, \quad \|u\|_{L^2(\Omega)} = (u, u)_{L^2(\Omega)}^{\frac{1}{2}}.$$

Definition 2.1 (Left and right fractional derivative spaces). For constant $\mu > 0$, define norms

$$\|u\|_{J_L^\mu(\Omega)} := (\|u\|_{L^2(\Omega)}^2 + \|{}_x D_L^\mu u\|_{L^2(\Omega)}^2)^{\frac{1}{2}}, \quad \|u\|_{J_R^\mu(\Omega)} := (\|u\|_{L^2(\Omega)}^2 + \|{}_x D_R^\mu u\|_{L^2(\Omega)}^2)^{\frac{1}{2}},$$

and let $J_{L,0}^\mu(\Omega)$ and $J_{R,0}^\mu(\Omega)$ be closures of $C_0^\infty(\Omega)$ under $\|\cdot\|_{J_L^\mu(\Omega)}$ and $\|\cdot\|_{J_R^\mu(\Omega)}$, respectively.

Definition 2.2 (Fractional Sobolev space). For constant $\mu > 0$, define the norm

$$\|u\|_{H^\mu(\Omega)} := \|\bar{u}\|_{H^\mu(\mathbb{R})} = \left[\int_{\mathbb{R}} (1+|\xi|^2)^\mu |\bar{u}(\xi)|^2 d\xi \right]^{\frac{1}{2}}$$

and let $H_0^\mu(\Omega)$ be the closure of $C_0^\infty(\Omega)$ under $\|\cdot\|_{H^\mu(\Omega)}$, where \bar{u} is the extension of u by zero from Ω to the entire x -axis, and \bar{u} is the Fourier transform of \bar{u} .

Lemma 2.1 (see [13], Proposition 1). If constant $\mu \in (0,1)$, $u, v \in J_{L,0}^{2\mu}(\Omega)$ (or $J_{R,0}^{2\mu}(\Omega)$), then

$$({}_x D_L^{2\mu} u, v)_{L^2(\Omega)} = ({}_x D_L^\mu u, {}_x D_R^\mu v)_{L^2(\Omega)}, \quad ({}_x D_R^{2\mu} u, v)_{L^2(\Omega)} = ({}_x D_R^\mu u, {}_x D_L^\mu v)_{L^2(\Omega)}.$$

Lemma 2.2 (see [12], Lemma 2.4). *For constant $\mu > 0$, we have*

$$({}_x D_L^\mu u, {}_x D_R^\mu u)_{L^2(\Omega)} = \cos(\pi\mu) \|{}_x D_L^\mu u\|_{L^2(\Omega)}^2. \tag{2.1}$$

Lemma 2.3 (Fractional Poincaré-Friedrichs inequality, see [12], Theorem 2.10). *For $u \in J_{L,0}^\mu(\Omega)$, we have*

$$\|u\|_{L^2(\Omega)} \lesssim \|{}_x D_L^\mu u\|_{L^2(\Omega)}. \tag{2.2}$$

2.2 Derivation of the fully discrete scheme

By Lemma 2.1, we get the variational (weak) formulation of (1.1a)-(1.1c): given $f \in L^2(\Omega, I)$, $\psi_0 \in L^2(\Omega)$ and $Q_t := \Omega \times (0, t)$, to find $u \in \mathcal{H}$ subject to $u(x, 0) = \psi_0(x)$ and

$$\left({}_0^C D_\sigma^\alpha u, v \right)_{Q_t} + B_\Omega^t(u, v) = (f, v)_{Q_t}, \quad \forall v \in \mathcal{H}^*, \tag{2.3}$$

where $\mathcal{H} := H_0^\beta(\Omega) \times H^1(I)$, $\mathcal{H}^* := H_0^\beta(\Omega) \times L^2(I)$ and

$$\begin{aligned} \left({}_0^C D_\sigma^\alpha u, v \right)_{Q_t} &= \int_0^t \left({}_0^C D_\sigma^\alpha u, v \right)_{L^2(\Omega)} d\sigma, & (f, v)_{Q_t} &= \int_0^t (f, v)_{L^2(\Omega)} d\sigma, \\ B_\Omega^t(u, v) &= \int_0^t \frac{1}{2\cos(\beta\pi)} \left[({}_x D_L^\beta u, {}_x D_R^\beta v)_{L^2(\Omega)} + ({}_x D_R^\beta u, {}_x D_L^\beta v)_{L^2(\Omega)} \right] d\sigma. \end{aligned}$$

In order to acquire numerical solutions of u , we firstly make a (possibly nonuniform) temporal discretization by points $0 = t_0 < t_1 < \dots < t_N = T$, and a uniform spatial discretization by points $x_i = a + ih$, ($i = 0, 1, \dots, M$), where $h = (b - a) / M$ represents the space step size. Let $I_n = (t_{n-1}, t_n)$, $\tilde{I}_n = (0, t_n)$, $\tau_j = t_j - t_{j-1}$, $n = 1, 2, \dots, N$ and $\Omega_h = \{\Omega_l : \Omega_l = (x_{l-1}, x_l), l = 1, 2, \dots, M\}$.

We observe that it is convenient to form the FE spaces in tensor products

$$\mathcal{V}_n = \mathcal{V}_h^\beta(\Omega_h) \times \mathcal{V}_\tau(\tilde{I}_n), \quad \mathcal{V}_n^* = \mathcal{V}_h^\beta(\Omega_h) \times \mathcal{V}_\tau^*(I_n),$$

where

$$\begin{aligned} \mathcal{V}_h^\beta(\Omega_h) &= \{w_h \in H_0^\beta(\Omega) \cap C(\bar{\Omega}) : w_h(x)|_{\Omega_l} \in \mathcal{P}_1(\Omega_l), l = 1, \dots, M\}, \\ \mathcal{V}_\tau(\tilde{I}_n) &= \{v_\tau \in C(\bar{I}_n) : v_\tau(0) = 1, v_\tau(t)|_{I_j} \in \mathcal{P}_1(I_j), j = 1, \dots, n\}, \\ \mathcal{V}_\tau^*(I_n) &= \{v_\tau \in L^2(I_n) : v_\tau(t)|_{I_n} \in \mathcal{P}_0(I_n)\}, \end{aligned}$$

and \mathcal{P}_k denotes the set of all polynomials of degree $\leq k$.

Remark 2.1. Apparently, for a given $u_{h\tau}(x, t) \in \mathcal{V}_n$, we have $\partial u_{h\tau} / \partial t \in \mathcal{V}_n^*$, where $\partial u_{h\tau} / \partial t$ is obtained by differentiating $u_{h\tau}$ with respect to t on each subinterval I_j , ($j = 1, 2, \dots, N$).

We obtain a fully discrete FE scheme in temporal and spatial directions of problem (2.3): given $Q_n := \Omega_h \times I_n$, to find $u_{h\tau} \in \mathcal{V}_n$ such that $u_{h\tau}(x, 0) = \psi_{0,I}(x)$ and

$$\left({}_0^C D_t^\alpha u_{h\tau}, v_{h\tau} \right)_{Q_n} + B_\Omega^n(u_{h\tau}, v_{h\tau}) = (f, v_{h\tau})_{Q_n}, \quad \forall v_{h\tau} \in \mathcal{V}_n^*, \tag{2.4}$$

where $\psi_{0,I}(x) \in \mathcal{V}_n$ satisfying $\psi_{0,I}(x_i) = \psi_0(x_i)$, $(i = 0, 1, \dots, M)$ and

$$\begin{aligned} \left({}_0^C D_t^\alpha u_{h\tau}, v_{h\tau} \right)_{Q_n} &= \int_{t_{n-1}}^{t_n} \left({}_0^C D_t^\alpha u_{h\tau}, v_{h\tau} \right)_{L^2(\Omega)} dt, \quad (f, v_{h\tau})_{Q_n} = \int_{t_{n-1}}^{t_n} (f, v_{h\tau})_{L^2(\Omega)} dt, \\ B_\Omega^n(u_{h\tau}, v_{h\tau}) &= \int_{t_{n-1}}^{t_n} \frac{1}{2\cos(\beta\pi)} \left[({}_x D_L^\beta u_{h\tau}, {}_x D_R^\beta v_{h\tau})_{L^2(\Omega)} + ({}_x D_R^\beta u_{h\tau}, {}_x D_L^\beta v_{h\tau})_{L^2(\Omega)} \right] dt. \end{aligned}$$

Let

$$\begin{aligned} \mathcal{L}_0(t) &= \begin{cases} \frac{t_1-t}{\tau_1}, & t \in I_1, \\ 0, & t \in \tilde{I}_n \setminus I_1, \end{cases} & \tilde{\mathcal{L}}_0(t) &= \frac{1}{\Gamma(1-\alpha)} \int_{t_0}^t \frac{d\mathcal{L}_0(s)}{(t-s)^\alpha}, & \hat{\mathcal{L}}_0(t) &= \frac{1}{\Gamma(1-\alpha)} \int_{t_0}^{t_1} \frac{d\mathcal{L}_0(s)}{(t-s)^\alpha}, \\ \mathcal{L}_k(t) &= \begin{cases} \frac{t_{k+1}-t}{\tau_{k+1}}, & t \in I_{k+1}, \\ \frac{t-t_{k-1}}{\tau_k}, & t \in I_k, \\ 0, & t \in \tilde{I}_n \setminus (I_k \cup I_{k+1}), \end{cases} & \hat{\mathcal{L}}_k(t) &= \frac{1}{\Gamma(1-\alpha)} \int_{t_{k-1}}^{t_{k+1}} \frac{d\mathcal{L}_k(s)}{(t-s)^\alpha}, \quad k=1, \dots, n-1, \end{aligned}$$

and

$$\mathcal{L}_n(t) = \begin{cases} \frac{t-t_{n-1}}{\tau_n}, & t \in I_n, \\ 0, & t \in \tilde{I}_n \setminus I_n, \end{cases} \quad \tilde{\mathcal{L}}_n(t) = \frac{1}{\Gamma(1-\alpha)} \int_{t_{n-1}}^t \frac{d\mathcal{L}_n(s)}{(t-s)^\alpha}.$$

Note that

$$\mathcal{V}_n^* = \text{span}\{\phi_l(x) \times 1, l = 1, \dots, M-1\},$$

where $\phi_l(x)$ is the shape function at $x_l \in \Omega_h$. Using

$$u_{h\tau}(x, t) = \sum_{k=0}^n u_h^k(x) \mathcal{L}_k(t),$$

we have

$$\left({}_0^C D_t^\alpha u_{h\tau}, \phi_l \times 1 \right)_{Q_1} = (u_h^0, \phi_l)_{L^2(\Omega)} (\tilde{\mathcal{L}}_0, 1)_{L^2(I_1)} + (u_h^1, \phi_l)_{L^2(\Omega)} (\tilde{\mathcal{L}}_1, 1)_{L^2(I_1)}, \tag{2.5a}$$

$$\left({}_0^C D_t^\alpha u_{h\tau}, \phi_l \times 1 \right)_{Q_n} = \sum_{k=0}^{n-1} (u_h^k, \phi_l)_{L^2(\Omega)} (\hat{\mathcal{L}}_k, 1)_{L^2(I_n)} + (u_h^n, \phi_l)_{L^2(\Omega)} (\tilde{\mathcal{L}}_n, 1)_{L^2(I_n)}, \quad n > 1, \tag{2.5b}$$

$$\int_{t_{n-1}}^{t_n} 1 \times ({}_x D_L^\beta u_{h\tau}, {}_x D_R^\beta \phi_l)_{L^2(\Omega)} dt = \sum_{k=0}^n ({}_x D_L^\beta u_h^k, {}_x D_R^\beta \phi_l)_{L^2(\Omega)} (\mathcal{L}_k, 1)_{L^2(I_n)}, \tag{2.5c}$$

$$\int_{t_{n-1}}^{t_n} 1 \times ({}_x D_R^\beta u_{h\tau}, {}_x D_L^\beta \phi_l)_{L^2(\Omega)} dt = \sum_{k=0}^n ({}_x D_R^\beta u_h^k, {}_x D_L^\beta \phi_l)_{L^2(\Omega)} (\mathcal{L}_k, 1)_{L^2(I_n)}. \tag{2.5d}$$

Substituting (2.5a)-(2.5d) into (2.4), yields

$$C_{h\tau}^n U_{h\tau}^n = G_{h\tau}^n, \tag{2.6}$$

where the coefficient matrix

$$C_{h\tau}^n = M_h + \frac{\Gamma(3-\alpha)}{2} \tau_n^\alpha A_h^\beta, \tag{2.7}$$

the right-hand side vector

$$G_{h\tau}^n = \Gamma(3-\alpha) \tau_n^{\alpha-1} F_{h\tau}^n + \left[M_h - \frac{\Gamma(3-\alpha)}{2} \tau_n^\alpha A_h^\beta \right] U_{h\tau}^{n-1} - \sum_{k=1}^{n-1} \tau_n^{\alpha-1} \times \frac{(t_n - t_{k-1})^{2-\alpha} - (t_{n-1} - t_{k-1})^{2-\alpha} - (t_n - t_k)^{2-\alpha} + (t_{n-1} - t_k)^{2-\alpha}}{\tau_k} M_h (U_{h\tau}^k - U_{h\tau}^{k-1}),$$

the mass matrix

$$M_h = \frac{h}{6} \begin{pmatrix} 4 & 1 & & & \\ 1 & 4 & 1 & & \\ & \ddots & \ddots & \ddots & \\ & & 1 & 4 & 1 \\ & & & 1 & 4 \end{pmatrix}_{(M-1) \times (M-1)}, \tag{2.8}$$

the stiffness matrix $A_h^\beta = (a_{i,j}^h)_{(M-1) \times (M-1)}$ with its entries

$$\begin{cases} a_{i,i}^h = \frac{h^{1-2\beta}(2^{4-2\beta}-8)}{2\cos(\beta\pi)\Gamma(4-2\beta)}, & i=1, \dots, M-1, \\ a_{j,j+1}^h = a_{j+1,j}^h = \frac{h^{1-2\beta}(3^{3-2\beta}-2^{5-2\beta}+7)}{2\cos(\beta\pi)\Gamma(4-2\beta)}, & j=1, \dots, M-2, \\ a_{k,k+l}^h = a_{k+l,k}^h = \frac{h^{1-2\beta}}{2\cos(\beta\pi)\Gamma(4-2\beta)} [(l+2)^{3-2\beta} - 4(l+1)^{3-2\beta} + 6l^{3-2\beta} - 4(l-1)^{3-2\beta} + (l-2)^{3-2\beta}], & k=1, \dots, M-l-1, \end{cases} \tag{2.9}$$

the vector

$$F_{h\tau}^n = (f_1^n, f_2^n, \dots, f_{M-1}^n)^T, \quad f_l^n = (f, \phi_l \times 1)_{Q_n}, \quad l=1, \dots, M-1,$$

and the fully discrete FE approximations

$$U_{h\tau}^k = (u_1^k, u_2^k, \dots, u_{M-1}^k)^T, \quad u_j^0 = \psi_{0,l}(x_j), \quad u_j^k = u_h^k(x_j), \quad k=1, \dots, n, \quad j=1, \dots, M-1.$$

Remark 2.2. (2.6) is reduced via dividing both sides of (2.4) by the factor $\tau_n^{1-\alpha} / \Gamma(3-\alpha)$, in case of the severe loss in convergence of the fully discrete FE scheme.

Next, a number of characterizations are established regarding A_h^β just defined by (2.9).

Theorem 2.1. *The stiffness matrix A_h^β is symmetric and satisfies*

1. $a_{i,i}^h > 0$ for $i = 1, \dots, M-1$;
2. $a_{i,j}^h < 0$ for $i \neq j, i, j = 1, \dots, M-1$;
3. $\sum_{j=1}^{M-1} a_{i,j}^h > 0$ for $i = 1, \dots, M-1$.

As a result, A_h^β is an M-matrix. Moreover, for the particular case when $h \leq 1/7$, we have

$$\sum_{j=1}^{M-1} a_{i,j}^h \geq \begin{cases} -\frac{h^{1-2\beta}(4-2^{3-2\beta})}{2\cos(\beta\pi)\Gamma(4-2\beta)}, & i = 1, M-1, \\ -\frac{2^{2\beta}h(2\beta-1)}{\cos(\beta\pi)\Gamma(2-2\beta)}, & i = 2, \dots, M-2. \end{cases} \quad (2.10)$$

Proof. The symmetric property of A_h^β is an obvious fact by (2.9). Since $\beta \in (1/2, 1)$, then $4-2\beta < 3$ and $\cos(\beta\pi) < 0$, which give immediately $a_{i,i}^h > 0, i = 1, \dots, M-1$. This proves the first part of the theorem. The second part is an immediate consequence of the facts that on the interval $\beta \in (1/2, 1)$, $f(\beta) = 3^{3-2\beta} - 2^{5-2\beta} + 7$ is a strictly increasing function and the bivariate function

$$f_\beta(l) = (l+2)^{3-2\beta} - 4(l+1)^{3-2\beta} + 6l^{3-2\beta} - 4(l-1)^{3-2\beta} + (l-2)^{3-2\beta} > 0$$

for $2 \leq l \leq M-2$. In fact, it is evident that

$$1.5^{2\beta} > 1.5 > \frac{3^3 \ln 3}{2^5 \ln 2} \Rightarrow f'(\beta) = -2\ln 3 \cdot 3^{3-2\beta} + 2\ln 2 \cdot 2^{5-2\beta} > 0,$$

and

$$f_\beta(l) = h^{2\beta-3} [g(x_{l+2}) - 4g(x_{l+1}) + 6g(x_l) - 4g(x_{l-1}) + g(x_{l-2})] > 0$$

using Taylor's expansion with

$$\left(\frac{l}{l+1}\right)^{2+2\beta} - \left(\frac{l}{l-1}\right)^{2+2\beta} > -\frac{30l}{2\beta+1} \Rightarrow l^{-1-2\beta} + \frac{2\beta+1}{30} [(l+1)^{-2-2\beta} - (l-1)^{-2-2\beta}] > 0,$$

where $g(x) = (x-a)^{3-2\beta}$ and $x_l = lh+a$.

To prove the third part, use

$$({}_x D_L^\beta \phi_i, {}_x D_R^\beta \phi_j)_{L^2(\Omega)} = - \left({}_x D_L^{2\beta-1} \phi_i, \frac{d\phi_j}{dx} \right)_{L^2(\Omega)}$$

and

$$\tilde{\phi} := \sum_{j=1}^{M-1} \phi_j = 1 - \phi_0 - \phi_M$$

to obtain the relation

$$\sum_{j=1}^{M-1} a_{i,j}^h = - \frac{(x D_L^{2\beta-1} \tilde{\phi}, 1)_{\Omega_i} - (x D_L^{2\beta-1} \tilde{\phi}, 1)_{\Omega_{i+1}} + (x D_L^{2\beta-1} \phi_i, 1)_{\Omega_1} - (x D_L^{2\beta-1} \phi_i, 1)_{\Omega_M}}{2h \cos(\beta\pi)},$$

where

$$x D_L^{2\beta-1} \tilde{\phi} = \begin{cases} \frac{(x-a)^{2-2\beta}}{h\Gamma(3-2\beta)}, & a < x < x_1, \\ \frac{(x-a)^{2-2\beta} - (x-x_1)^{2-2\beta}}{h\Gamma(3-2\beta)}, & x_1 < x < x_{M-1}, \\ \frac{(x-a)^{2-2\beta} - (x-x_1)^{2-2\beta} - (x-x_{M-1})^{2-2\beta}}{h\Gamma(3-2\beta)}, & x_{M-1} < x < x_M, \end{cases}$$

and

$$x D_L^{2\beta-1} \phi_i(x) = \begin{cases} 0, & x < x_{i-1}, \\ \frac{(x-x_{i-1})^{2-2\beta}}{h\Gamma(3-2\beta)}, & x_{i-1} < x < x_i, \\ \frac{(x-x_{i-1})^{2-2\beta} - 2(x-x_i)^{2-2\beta}}{h\Gamma(3-2\beta)}, & x_i < x < x_{i+1}, \\ \frac{(x-x_{i-1})^{2-2\beta} - 2(x-x_i)^{2-2\beta} + (x-x_{i+1})^{2-2\beta}}{h\Gamma(3-2\beta)}, & x > x_{i+1}. \end{cases}$$

Assume that $\Omega = (0,1)$ without loss of generality, one can easily derive

$$\sum_{j=1}^{M-1} a_{i,j}^h = - \frac{(4-2^{3-2\beta})h^{3-2\beta} - 1 + 3(1-h)^{3-2\beta} - 3(1-2h)^{3-2\beta} + (1-3h)^{3-2\beta}}{2\cos(\beta\pi)h^2\Gamma(4-2\beta)}$$

for $i=1, M-1$,

$$\sum_{j=1}^{M-1} a_{i,j}^h = - \frac{3(ih)^{3-2\beta} - 3[(i-1)h]^{3-2\beta} + [(i-2)h]^{3-2\beta} - [(i+1)h]^{3-2\beta}}{2\cos(\beta\pi)h^2\Gamma(4-2\beta)} - \frac{3(1-ih)^{3-2\beta} - [1-(i-1)h]^{3-2\beta} - 3[1-(i+1)h]^{3-2\beta} + [1-(i+2)h]^{3-2\beta}}{2\cos(\beta\pi)h^2\Gamma(4-2\beta)}$$

for $i=2, \dots, M-2$ and deduce $\sum_{j=1}^{M-1} a_{i,j}^h > 0$ by Taylor's formula and $\beta \in (1/2, 1)$.

Another step to do in the proof is that A_h^β is an M-matrix. According to Properties 1 and 2, this result will be proved by showing that $(A_h^\beta)^{-1}$ is nonnegative, which can be easily proved by contradiction with the Property 3.

Finally, to prove (2.10), which follows from

$$h \leq 1/7 \Rightarrow 7 - 4(1 - \xi)^{-1-2\beta} > -\frac{1}{\beta h} \Rightarrow -1 + 3(1 - h)^{3-2\beta} - 3(1 - 2h)^{3-2\beta} + (1 - 3h)^{3-2\beta} > 0$$

for all $\xi \in (0, 2h)$,

$$\left(\frac{i-1}{i}\right)^{3+2\beta} > \frac{\beta+1}{21(\beta+1)+30i} \Rightarrow \frac{3(ih)^{3-2\beta} - 3(ih-h)^{3-2\beta} + (ih-2h)^{3-2\beta} - (ih+h)^{3-2\beta}}{h^3(3-2\beta)(2-2\beta)(2\beta-1)(ih)^{-2\beta}} > 1$$

and

$$\frac{3(1-ih)^{3-2\beta} - [1-(i-1)h]^{3-2\beta} - 3[1-(i+1)h]^{3-2\beta} + [1-(i+2)h]^{3-2\beta}}{h^3(3-2\beta)(2-2\beta)(2\beta-1)(1-ih)^{-2\beta}} > 1$$

for $i = 2, \dots, M-2$, together with the inequality $(ih)^{-2\beta} + (1-ih)^{-2\beta} \geq 2^{1+2\beta}$. □

Observe from (2.8)-(2.9) that M_h and A_h^β are both symmetric Toeplitz matrices independent of any time terms. The under-mentioned corollaries are natural consequences of Theorem 2.1.

Corollary 2.1. *The coefficient matrix $C_{h\tau}^n$ is a symmetric Toeplitz matrix. Furthermore, it will be independent of time level n if the temporal discretization is also uniform.*

Corollary 2.2. *The coefficient matrix $C_{h\tau}^n$ is an M-matrix, if and only if*

$$\frac{\tau_n^\alpha}{h^{2\beta}} > -\frac{2\cos(\beta\pi)\Gamma(4-2\beta)}{3\Gamma(3-\alpha)(3^{3-2\beta}-2^{5-2\beta}+7)}. \tag{2.11}$$

Proof. This result will follow from Theorem 2.1, if we can show that

$$\frac{h}{6} + \frac{\Gamma(3-\alpha)}{2} \tau_n^\alpha \frac{h^{1-2\beta}(3^{3-2\beta}-2^{5-2\beta}+7)}{2\cos(\beta\pi)\Gamma(4-2\beta)} < 0,$$

which is an immediate application of the condition (2.11). □

2.3 Numerical experiments and the saturation error order

Example 2.1. Consider (1.1a)-(1.1c) with $\Omega = (0, 1)$, $T = 1$, $\psi_0(x) = 0$ and

$$f(x, t) = \frac{\Gamma(3-\alpha)}{\Gamma(3-2\alpha)} t^{2-2\alpha} x^2 (1-x)^2 + \frac{t^{2-\alpha}}{\cos(\beta\pi)} \left[\frac{x^{2-2\beta} + (1-x)^{2-2\beta}}{\Gamma(3-2\beta)} - \frac{6x^{3-2\beta} + 6(1-x)^{3-2\beta}}{\Gamma(4-2\beta)} + \frac{12x^{4-2\beta} + 12(1-x)^{4-2\beta}}{\Gamma(5-2\beta)} \right].$$

Table 1: Error results and convergence rates in spatial direction with $h = \tau$.

N	$\beta = 0.6$						$\beta = 0.8$					
	$\alpha = 0.01$		$\alpha = 0.50$		$\alpha = 0.99$		$\alpha = 0.01$		$\alpha = 0.50$		$\alpha = 0.99$	
	$\ e\ _0$	rate	$\ e\ _0$	rate	$\ e\ _0$	rate	$\ e\ _0$	rate	$\ e\ _0$	rate	$\ e\ _0$	rate
8	8.94E-4	-	8.78E-4	-	8.88E-4	-	9.73E-4	-	9.56E-4	-	9.72E-4	-
16	2.02E-4	2.15	1.98E-4	2.15	2.00E-4	2.15	2.34E-4	2.06	2.29E-4	2.06	2.33E-4	2.06
32	4.49E-5	2.17	4.42E-5	2.16	4.47E-5	2.16	5.51E-5	2.08	5.40E-5	2.08	5.49E-5	2.08
64	1.01E-5	2.15	1.00E-5	2.14	1.01E-5	2.14	1.30E-5	2.09	1.27E-5	2.09	1.29E-5	2.09
N	$\alpha = 0.10$		$\alpha = 0.25$		$\alpha = 0.75$		$\alpha = 0.10$		$\alpha = 0.25$		$\alpha = 0.75$	
	$\ e\ _0$	rate	$\ e\ _0$	rate	$\ e\ _0$	rate	$\ e\ _0$	rate	$\ e\ _0$	rate	$\ e\ _0$	rate
	8	8.90E-4	-	8.80E-4	-	8.83E-4	-	9.72E-4	-	9.63E-4	-	9.64E-4
16	1.99E-4	2.16	1.97E-4	2.16	1.99E-4	2.15	2.31E-4	2.07	2.28E-4	2.08	2.31E-4	2.06
32	4.39E-5	2.18	4.40E-5	2.16	4.44E-5	2.16	5.39E-5	2.10	5.34E-5	2.09	5.44E-5	2.09
64	9.95E-6	2.14	1.00E-5	2.14	1.01E-5	2.14	1.25E-5	2.11	1.26E-5	2.08	1.28E-5	2.09

Table 2: Error results and convergence rates in spatial direction with $h = \sqrt{\tau}$.

N	$\beta = 0.6$						$\beta = 0.8$					
	$\alpha = 0.01$		$\alpha = 0.50$		$\alpha = 0.99$		$\alpha = 0.01$		$\alpha = 0.50$		$\alpha = 0.99$	
	$\ e\ _0$	rate	$\ e\ _0$	rate	$\ e\ _0$	rate	$\ e\ _0$	rate	$\ e\ _0$	rate	$\ e\ _0$	rate
16	3.64E-3	-	3.63E-3	-	3.63E-3	-	3.76E-3	-	3.75E-3	-	3.75E-3	-
64	8.94E-4	1.01	8.87E-4	1.02	8.88E-4	1.02	9.73E-4	0.97	9.69E-4	0.98	9.72E-4	0.98
256	2.02E-4	1.07	2.00E-4	1.08	2.00E-4	1.08	2.34E-4	1.03	2.32E-4	1.03	2.33E-4	1.03
N	$\alpha = 0.10$		$\alpha = 0.25$		$\alpha = 0.75$		$\alpha = 0.10$		$\alpha = 0.25$		$\alpha = 0.75$	
	$\ e\ _0$	rate	$\ e\ _0$	rate	$\ e\ _0$	rate	$\ e\ _0$	rate	$\ e\ _0$	rate	$\ e\ _0$	rate
	16	3.64E-3	-	3.63E-3	-	3.63E-3	-	3.75E-3	-	3.75E-3	-	3.75E-3
64	8.90E-4	1.02	8.87E-4	1.02	8.86E-4	1.02	9.72E-4	0.98	9.71E-4	0.98	9.69E-4	0.98
256	2.01E-4	1.07	2.01E-4	1.07	2.00E-4	1.08	2.33E-4	1.03	2.33E-4	1.03	2.32E-4	1.03

The exact solution is $u(x,t) = t^{2-\alpha}x^2(1-x)^2$. In the case of uniform temporal and spatial meshes ($\tau=1/N, h=1/M$), Tables 1 and 2 present errors $\|e\|_0 := \|u(\cdot, 1) - u_{h\tau}(\cdot, 1)\|_{L^2(\Omega)}$ and convergence rates.

From Tables 1 and 2, we can obtain that the fully discrete FE solution $u_{h\tau}$ achieves the saturation error order $\mathcal{O}(\tau^2 + h^2)$ under $\|\cdot\|_0$ norm.

Fig. 1 illustrates the comparisons of exact solutions and numerical solutions of $\alpha=0.2, 0.4$ and $\beta=0.6, 0.8$ with $t=1$ and $h = \tau = 1/32$.

3 Condition number estimation

This section is devoted to deriving the condition number estimation on the coefficient matrix of (2.6) in uniform temporal (step size denoted by τ) and spatial discretizations.

Theorem 3.1. For the linear system (2.6), we have

$$\kappa(C_{h\tau}^n) \lesssim 1 + \tau^\alpha h^{-2\beta}. \tag{3.1}$$

Proof. Let $C_\alpha = \Gamma(3-\alpha)/2$, we divide our proof in three steps. First, it is trivially true that

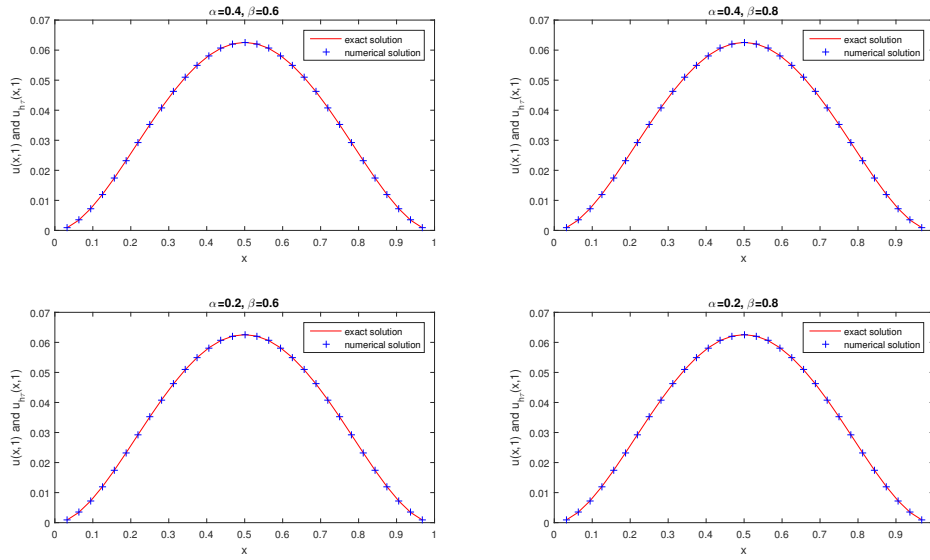


Figure 1: Comparisons on exact solutions and numerical solutions with $t=1$ and $h=\tau=1/32$.

$C_{h\tau}^n$ is spectrally equivalent to the matrix $I + C_\alpha \tau^\alpha M_h^{-\frac{1}{2}} A_h^\beta M_h^{-\frac{1}{2}}$, i.e.,

$$\kappa(C_{h\tau}^n) \simeq \kappa\left(I + C_\alpha \tau^\alpha M_h^{-\frac{1}{2}} A_h^\beta M_h^{-\frac{1}{2}}\right). \tag{3.2}$$

The next thing to do in the proof is to verify

$$\lambda_{\min}(M_h^{-\frac{1}{2}} A_h^\beta M_h^{-\frac{1}{2}}) \gtrsim 1, \quad \lambda_{\max}(M_h^{-\frac{1}{2}} A_h^\beta M_h^{-\frac{1}{2}}) \lesssim h^{-2\beta}, \tag{3.3}$$

which is equivalent to

$$(\vec{v}_h, \vec{v}_h) \lesssim (M_h^{-\frac{1}{2}} A_h^\beta M_h^{-\frac{1}{2}} \vec{v}_h, \vec{v}_h) \lesssim h^{-2\beta} (\vec{v}_h, \vec{v}_h), \quad \forall \vec{v}_h \in \mathbb{R}^{M-1}. \tag{3.4}$$

Set $\vec{u}_h = M_h^{-\frac{1}{2}} \vec{v}_h := (u_1^h, \dots, u_{M-1}^h)^T$, rewrite (3.4) as $(M_h \vec{u}_h, \vec{u}_h) \lesssim (A_h^\beta \vec{u}_h, \vec{u}_h) \lesssim h^{-2\beta} (M_h \vec{u}_h, \vec{u}_h)$. It is sufficient to verify that $(M_h \vec{u}_h, \vec{u}_h) \simeq h(\vec{u}_h, \vec{u}_h)$. It follows by (2.8) and the Cauchy-Schwarz inequality that

$$\frac{h}{3} (\vec{u}_h, \vec{u}_h) \leq (M_h \vec{u}_h, \vec{u}_h) = h \left[\frac{2}{3} \sum_{l=1}^{M-1} (u_l^h)^2 + \frac{1}{3} \sum_{l=1}^{M-2} u_l^h u_{l+1}^h \right] \leq h(\vec{u}_h, \vec{u}_h).$$

Thus (3.3) will follow if we can show that $h(\vec{u}_h, \vec{u}_h) \lesssim (A_h^\beta \vec{u}_h, \vec{u}_h) \lesssim h^{1-2\beta} (\vec{u}_h, \vec{u}_h)$. We start by showing the second inequality. Utilizing Theorem 2.1 and the Cauchy-Schwarz in-

equality, we arrive at

$$\begin{aligned}
 (A_h^\beta \vec{u}_h, \vec{u}_h) &\leq \sum_{i=1}^{M-1} a_{i,i}^h (u_i^h)^2 - \frac{1}{2} \sum_{i=1}^{M-1} \sum_{j \neq i}^{M-1} a_{i,j}^h [(u_i^h)^2 + (u_j^h)^2] \\
 &= \sum_{i=1}^{M-1} a_{i,i}^h (u_i^h)^2 - \sum_{i=1}^{M-1} \sum_{j=i+1}^{M-1} a_{i,j}^h (u_i^h)^2 - \sum_{i=1}^{M-1} \sum_{j=i+1}^{M-1} a_{i,j}^h (u_j^h)^2 \\
 &= \sum_{i=1}^{M-1} (u_i^h)^2 \left[a_{i,i}^h - \sum_{j=i+1}^{M-1} a_{i,j}^h - \sum_{j=1}^{i-1} a_{i,j}^h \right] \\
 &\leq 2a_{1,1}^h (\vec{u}_h, \vec{u}_h) = \frac{(2^{4-2\beta} - 8)}{\cos(\beta\pi)\Gamma(4-2\beta)} h^{1-2\beta} (\vec{u}_h, \vec{u}_h),
 \end{aligned}$$

which proves the second inequality. To prove the left inequality, set $u_h := \Phi_h \vec{u}_h$, we rewrite it as

$$\frac{1}{\cos(\beta\pi)} ({}_x D_L^\beta u_h, {}_x D_R^\beta u_h)_{L^2(\Omega)} = (A_h^\beta \vec{u}_h, \vec{u}_h) \gtrsim h(\vec{u}_h, \vec{u}_h) \simeq (M_h \vec{u}_h, \vec{u}_h) = (u_h, u_h)_{L^2(\Omega)},$$

which can be deduced by (2.1)-(2.2), where $\Phi_h = (\phi_1, \dots, \phi_{M-1})$.

Finally, we have to show that

$$\begin{aligned}
 &\kappa \left(I + C_\alpha \tau^\alpha M_h^{-\frac{1}{2}} A_h^\beta M_h^{-\frac{1}{2}} \right) \\
 &= \frac{\lambda_{\max} \left(I + C_\alpha \tau^\alpha M_h^{-\frac{1}{2}} A_h^\beta M_h^{-\frac{1}{2}} \right)}{\lambda_{\min} \left(I + C_\alpha \tau^\alpha M_h^{-\frac{1}{2}} A_h^\beta M_h^{-\frac{1}{2}} \right)} = \frac{1 + C_\alpha \tau^\alpha \lambda_{\max} (M_h^{-\frac{1}{2}} A_h^\beta M_h^{-\frac{1}{2}})}{1 + C_\alpha \tau^\alpha \lambda_{\min} (M_h^{-\frac{1}{2}} A_h^\beta M_h^{-\frac{1}{2}})} \\
 &\leq 1 + C_\alpha \frac{(2^{4-2\beta} - 8)}{\cos(\beta\pi)\Gamma(4-2\beta)} \tau^\alpha h^{-2\beta}.
 \end{aligned}$$

This completes the proof based on the spectral equivalence relation (3.2). □

Remark 3.1. The estimation (3.1) is compatible with the correlative result $1 + \mathcal{O}(\tau h^{-2})$ of integer order parabolic differential equations.

An important particular case of Theorem 3.1 is singled out in the following corollary.

Corollary 3.1. *Let τ be proportional to h^μ with $\mu\alpha \geq 2\beta$. Then*

$$\kappa(C_{h\tau}^n) = \mathcal{O}(1). \tag{3.5}$$

In what follows, we examine the correctness of (3.1) concerning Example 2.1 with typical α and β for three specific cases: $\tau = h$, $\tau = h^2$ and τ is fixed (doesn't change along with h). In under-mentioned tables, λ_{\min} and λ_{\max} respectively indicate the smallest and largest eigenvalues, κ represents the condition number and *ratio* is the quotient of the condition number in fine grid divided by that in coarse grid.

It is observed from Tables 3-5 that numerical results are in good agreement with our theoretical estimation.

Table 3: The smallest and largest eigenvalues and condition numbers with $\tau = h$.

α	M	$\beta=0.6$				$\beta=0.8$			
		λ_{\min}	λ_{\max}	κ	ratio	λ_{\min}	λ_{\max}	κ	ratio
0.99	8	1.45E-1	1.97E-1	1.36E+0	-	1.63E-1	5.47E-1	3.35E+0	-
	16	6.81E-2	1.09E-1	1.60E+0	1.18	7.26E-2	4.11E-1	5.66E+0	1.69
	32	3.27E-2	6.03E-2	1.84E+0	1.15	3.39E-2	3.09E-1	9.12E+0	1.61
	64	1.60E-2	3.34E-2	2.09E+0	1.13	1.63E-2	2.33E-1	1.43E+1	1.57
0.5	8	2.09E-1	5.41E-1	2.59E+0	-	2.74E-1	1.89E+0	6.89E+0	-
	16	9.31E-2	4.25E-1	4.56E+0	1.76	1.16E-1	2.03E+0	1.74E+1	2.53
	32	4.22E-2	3.37E-1	8.00E+0	1.75	5.05E-2	2.17E+0	4.30E+1	2.47
	64	1.95E-2	2.70E-1	1.39E+1	1.73	2.24E-2	2.32E+0	1.04E+2	2.41
0.01	8	4.81E-1	2.08E+0	4.32E+0	-	7.50E-1	7.65E+0	1.02E+1	-
	16	2.42E-1	2.35E+0	9.69E+0	2.24	3.77E-1	1.17E+1	3.09E+1	3.03
	32	1.21E-1	2.66E+0	2.21E+1	2.28	1.88E-1	1.76E+1	9.36E+1	3.03
	64	6.00E-2	3.03E+0	5.06E+1	2.29	9.35E-2	2.65E+1	2.83E+2	3.03

Table 4: The smallest and largest eigenvalues and condition numbers with $\tau = h^2$.

α	M	$\beta=0.6$				$\beta=0.8$			
		λ_{\min}	λ_{\max}	κ	ratio	λ_{\min}	λ_{\max}	κ	ratio
0.5	8	1.52E-1	2.33E-1	1.53E+0	-	1.76E-1	6.96E-1	3.97E+0	-
	16	6.98E-2	1.30E-1	1.86E+0	1.21	7.57E-2	5.23E-1	6.91E+0	1.74
	32	3.31E-2	7.20E-2	2.17E+0	1.17	3.46E-2	3.92E-1	1.13E+1	1.64
	64	1.61E-2	4.01E-2	2.49E+0	1.15	1.65E-2	2.95E-1	1.79E+1	1.58
0.01	8	4.74E-1	2.04E+0	4.30E+0	-	7.37E-1	7.49E+0	1.02E+1	-
	16	2.37E-1	2.28E+0	9.62E+0	2.24	3.69E-1	1.13E+1	3.08E+1	3.02
	32	1.18E-1	2.57E+0	2.19E+1	2.27	1.83E-1	1.70E+1	9.30E+1	3.03
	64	5.82E-2	2.91E+0	5.00E+1	2.29	9.03E-2	2.54E+1	2.81E+2	3.03
β	8	1.40E-1	1.75E-1	1.24E+0	-	1.35E-1	2.00E-1	1.49E+0	-
	16	6.62E-2	8.84E-2	1.34E+0	1.07	6.42E-2	1.00E-1	1.56E+0	1.05
	32	3.21E-2	4.44E-2	1.38E+0	1.04	3.16E-2	5.00E-2	1.59E+0	1.02
	64	1.58E-2	2.22E-2	1.40E+0	1.02	1.57E-2	2.50E-2	1.60E+0	1.01

Table 5: The smallest and largest eigenvalues and the condition number with $\tau = 1/32$.

α	M	$\beta=0.6$				$\beta=0.8$			
		λ_{\min}	λ_{\max}	κ	ratio	λ_{\min}	λ_{\max}	κ	ratio
0.99	64	1.64E-2	5.83E-2	3.56E+0	1.93	1.69E-2	4.58E-1	2.70E+1	2.96
	128	8.19E-3	6.24E-2	7.62E+0	2.14	8.48E-3	6.89E-1	8.13E+1	3.01
	256	4.10E-3	6.97E-2	1.70E+1	2.23	4.24E-3	1.04E+0	2.46E+2	3.02
	512	2.05E-3	7.91E-2	3.86E+1	2.27	2.12E-3	1.58E+0	7.45E+2	3.03
0.5	64	2.11E-2	3.80E-1	1.80E+1	2.25	2.52E-2	3.28E+0	1.30E+2	3.02
	128	1.06E-2	4.33E-1	4.10E+1	2.28	1.26E-2	4.97E+0	3.94E+2	3.03
	256	5.27E-3	4.95E-1	9.39E+1	2.29	6.31E-3	7.53E+0	1.19E+3	3.03
	512	2.64E-3	5.68E-1	2.15E+2	2.29	3.16E-3	1.14E+1	3.62E+3	3.03
0.01	64	6.03E-2	3.05E+0	5.07E+1	2.29	9.40E-2	2.67E+1	2.84E+2	3.03
	128	3.01E-2	3.50E+0	1.16E+2	2.30	4.70E-2	4.05E+1	8.61E+2	3.03
	256	1.51E-2	4.02E+0	2.67E+2	2.30	2.35E-2	6.13E+1	2.61E+3	3.03
	512	7.53E-3	4.62E+0	6.14E+2	2.30	1.17E-2	9.29E+1	7.91E+3	3.03
β	M	$\alpha=0.01$				$\alpha=0.99$			
		λ_{\min}	λ_{\max}	κ	ratio	λ_{\min}	λ_{\max}	κ	ratio
0.999	64	1.63E-1	2.42E+2	1.49E+3	4.00	1.81E-2	4.11E+0	2.27E+2	3.98
	128	8.14E-2	4.84E+2	5.95E+3	4.00	9.06E-3	8.21E+0	9.07E+2	3.99
	256	4.07E-2	9.66E+2	2.38E+4	3.99	4.53E-3	1.64E+1	3.62E+3	3.99
	512	2.03E-2	1.93E+3	9.49E+4	3.99	2.27E-3	3.28E+1	1.45E+4	3.99

4 Classical AMG and an adaptive variant

Within the section, involving FFT to perform Toeplitz matrix-vector multiplications, we introduce the so-called Ruge-Stüben or classical AMG method [39,40] with low algorithmic complexity, fulfill its theoretical investigation, and then propose an adaptive AMG method through Corollary 3.1.

Algorithm 4.1. The classical AMG method for the linear system (2.6).

Step 1 Perform the Setup phase to the coefficient matrix $C_{h\tau}^n$.

- 1.1 Set the strength-of-connection tolerance θ ;
- 1.2 Build the ingredients required by a hierarchy of levels, coarsest to finest, including the grid transfer operators.

Step 2 Invoke the classical $V(\varrho_1, \varrho_2)$ -cycle to solve (2.6) until convergence. Underneath is the description of two-grid $V(\varrho_1, \varrho_2)$ -cycle, where P is the interpolation operator.

- 2.1 Do ϱ_1 pre-smoothing steps on (2.6);
- 2.2 Compute and restrict the residual: $r^c = P^T (G_{h\tau}^n - C_{h\tau}^n U_{h\tau}^n)$;
- 2.3 Solve the residual equation on coarse level: $(P^T C_{h\tau}^n P) e^c = r^c$;
- 2.4 Interpolation and correction: $U_{h\tau}^n = U_{h\tau}^n + P e^c$;
- 2.5 Do ϱ_2 post-smoothing steps on (2.6).

Remark 4.1. In pre- and post-smoothing processes, damped-Jacobi iterative methods are favorable choices, which can maintain the low computational cost $\mathcal{O}(M \log M)$ calculated by FFT.

For simplicity, we here denote $C_{h\tau}^n = (c_{ij})_{(M-1) \times (M-1)}$, and only consider the two-grid $V(0,1)$ -cycle, whose iteration matrix has the form

$$M_{h,H} = S[I - P(P^T C_{h\tau}^n P)^{-1} P^T C_{h\tau}^n],$$

where S is a relaxation operator usually chosen as damped-Jacobi or Gauss-Seidel iterative method.

For theoretical investigations, we rewrite (2.6) and P in block form regarding a given C/F splitting

$$C_{h\tau}^n U_{h\tau}^n = \begin{pmatrix} A_{FF} & A_{FC} \\ A_{CF} & A_{CC} \end{pmatrix} \begin{pmatrix} u_F \\ u_C \end{pmatrix} = \begin{pmatrix} f_F \\ f_C \end{pmatrix} = G_{h\tau}^n, \quad P = \begin{pmatrix} I_{FC} \\ I_{CC} \end{pmatrix},$$

and introduce the following inner products

$$(u_F, v_F)_{0,F} = (D_{FF} u_F, v_F), \quad (u, v)_1 = (C_{h\tau}^n u, v), \quad (u, v)_2 = (D_{h\tau}^{-1} C_{h\tau}^n u, C_{h\tau}^n v),$$

with their associated norms $\|\cdot\|_{0,F} = \sqrt{(\cdot, \cdot)_{0,F}}$ and $\|\cdot\|_i = \sqrt{(\cdot, \cdot)_i}$ ($i=1,2$), where I_{CC} is the identity operator, $D_{FF} = \mathbf{diag}(A_{FF})$ and $D_{h\tau} = \mathbf{diag}(C_{h\tau}^n)$.

Combining Corollary 2.2 and the two-level convergence theory in the work [41], leads to the following lemmas and theorem.

Lemma 4.1. *Under the condition (2.11), for all $e_h \in \mathbb{R}^{M-1}$, damped-Jacobi and Gauss-Seidel relaxations satisfy the smoothing property*

$$\|Se_h\|_1^2 \leq \|e_h\|_1^2 - \sigma_1 \|e_h\|_2^2 \tag{4.1}$$

with σ_1 independent of e_h and step sizes h and τ_n .

Proof. On the strength of Theorem A.3.1 and A.3.2 in [41], we produce that damped-Jacobi relaxation with parameter $0 < \omega < 2/\eta$ satisfies (4.1) with

$$\sigma_1 = \omega(2 - \omega\eta),$$

and Gauss-Seidel relaxation satisfies (4.1) with

$$\sigma_1 = \frac{1}{(1 + \gamma_-)(1 + \gamma_+)},$$

both independent of e_h , where

$$\eta \geq \rho(D_{h\tau}^{-1}C_{h\tau}^n), \quad \gamma_- = \max_i \left\{ \frac{1}{w_i c_{ii}} \sum_{j < i} w_j |c_{ij}| \right\}, \quad \gamma_+ = \max_i \left\{ \frac{1}{w_i c_{ii}} \sum_{j > i} w_j |c_{ij}| \right\},$$

and $w = (w_i)$ is an arbitrary positive vector with $C_{h\tau}^n w$ being also positive.

By exploiting (2.7)-(2.9), the assumption (2.11) and Corollary 2.2, we conclude that $C_{h\tau}^n$ is strictly diagonally dominant. Recall that $C_{h\tau}^n w$ is a positive vector, yield $\gamma_- < 1$, $\gamma_+ < 1$ and

$$\rho(D_{h\tau}^{-1}C_{h\tau}^n) \leq |D_{h\tau}^{-1}C_{h\tau}^n|_w = \max_i \left\{ \frac{1}{w_i} \sum_j w_j \frac{|c_{ij}|}{c_{ii}} \right\} < 2, \tag{4.2}$$

which implicitly mean that η , γ_- and γ_+ can be chosen to be independent of h and τ_n and complete the proof. □

Remark 4.2. The inequality (4.2) implies that there exists $\epsilon > 0$ such that $\rho(D_{h\tau}^{-1}C_{h\tau}^n) = 2 - 3\epsilon$. Then $\eta = 2 - 2\epsilon > \rho(D_{h\tau}^{-1}C_{h\tau}^n)$ and hence the upper bound of parameter ω : $2/\eta = 1/(1 - \epsilon) > 1$, which suggests that Jacobi relaxation with $\omega = 1$ is available in such a case.

Remark 4.3. For all symmetric M-matrices, $\sigma_1 \leq 1/\eta < 1$ holds for damped-Jacobi relaxation, while $\sigma_1 \in (1/4, 1)$ for Gauss-Seidel relaxation.

Lemma 4.2. Under the condition (2.11) and a given C/F splitting, for all $e_h = (e_F^T, e_C^T)^T \in \mathbb{R}^{M-1}$, the direct interpolation I_{FC} satisfies

$$\|e_F - I_{FC}e_C\|_{0,F}^2 \leq \sigma_2 \|e_h\|_1^2 \quad (4.3)$$

with σ_2 independent of e_h , h and τ_n .

Proof. According to Theorem A.4.3 in [41], I_{FC} satisfies (4.3) with σ_2 of the form regarding a given C/F splitting

$$\sigma_2 \geq \max_{i \in F} \left\{ \frac{\sum_{j \in N_i} c_{ij}}{\sum_{j \in C_i} c_{ij}} \right\} \quad (4.4)$$

independent of e_h , where $N_i = \{j \neq i : c_{ij} \neq 0\}$, C_i is the subset of N_i whose values will be used to interpolate at F -point i . As a result of (4.4) and the fact that c_{ij} ($j \in N_i$) are all negative, the following relation holds: $\sigma_2 > 1$.

Notice here that the classical Ruge-Stüben based coarsening strategy generates at least one of points $i-1$ and $i+1$ to be C -points and strongly influence i —viz. it retains $i-1 \in C_i$ or $i+1 \in C_i$. Therefore, it can be seen that

$$\frac{\sum_{j \in N_i} c_{ij}}{\sum_{j \in C_i} c_{ij}} < -\frac{c_{ii}}{c_{i-1}} = -\frac{c_{ii}}{c_{i+1}} = -\frac{16\cos(\beta\pi)\Gamma(4-2\beta) + 6\Gamma(3-\alpha)\tau_n^\alpha h^{-2\beta}(2^{4-2\beta}-8)}{4\cos(\beta\pi)\Gamma(4-2\beta) + 6\Gamma(3-\alpha)\tau_n^\alpha h^{-2\beta}(3^{3-2\beta}-2^{5-2\beta}+7)},$$

indicating that σ_2 is independent of h and τ_n by plugging (2.11) and thus prove the theorem. \square

Theorem 4.1. Let any C/F splitting be given. Under the condition (2.11), there exist positive constants σ_1 and σ_2 independent of h and τ_n and satisfying $\sigma_2 > 1 > \sigma_1$, such that a uniform two-grid convergence is achieved as follows

$$\|M_{h,H}\|_1 \leq \sqrt{1 - \sigma_1 / \sigma_2}.$$

Proof. The proof of this result is straightforward and is based on Theorems A.4.1 and A.4.2 in [41], Lemmas 4.1 and 4.2. \square

Now observe from Theorem 4.1 that, despite the independence of h and τ_n , σ_2 relies ruinously on θ in Step 1.1 of Algorithm 4.1 due to the fact that $C_{h\tau}^n$ is nearly dense leading to a quite complicated adjacency graph. In addition, it is found that $\sigma_2(\theta)$ may be much larger than 1 as θ approaches zero, with that comes a sharp pullback in convergence rate. Hence, an appropriate θ is a critical component of Algorithm 4.1 to handle fractional diffusion equations.

We now turn to reveal a reference formula on θ . Note the heuristic that the distribution of ratios of off-diagonal elements relative to the maximum absolute off-diagonal element (namely the minor diagonal element for $C_{h\tau}^n$) plays a major role in the choice of θ . Since $C_{h\tau}^n$ is a symmetric Toeplitz matrix from Corollary 2.1, its first row involving all

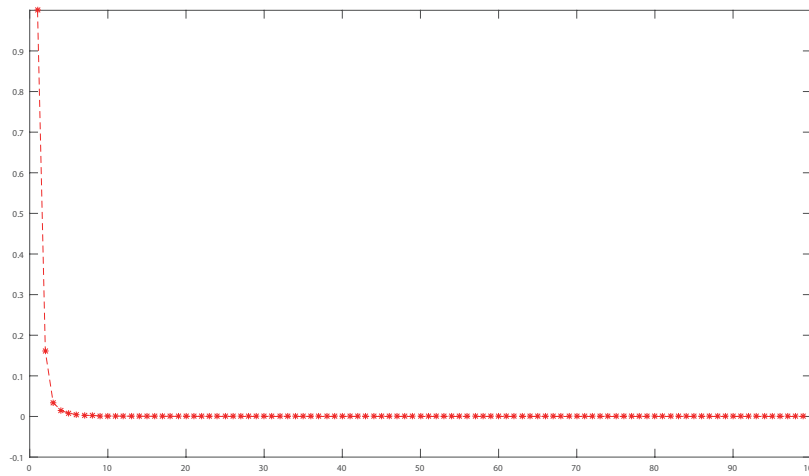


Figure 2: Distribution of ratios c_{1j}/c_{12} , $j=2,3,\dots,M-1$.

off-diagonal elements of $C_{h\tau}^n$ is deserved to be the representative row. Taking $\beta = 0.8$ as an example, Fig. 2 shows the distribution of the ratios c_{1j}/c_{12} ($j \geq 2$), which reminds us of the attenuation in off-diagonal elements, states

$$\frac{c_{13}}{c_{12}} \approx 0.160426, \quad \frac{c_{1j}}{c_{12}} < \frac{c_{14}}{c_{12}} \approx 0.034394, \quad j=5,6,\dots,M-1,$$

and suggests that c_{1j} ($j \geq 4$) should be viewed as weak couplings (wouldn't be used for interpolation) because they are less than 5% of c_{12} . Besides, for a better complexity and higher efficiency, only the nearest neighbors are potentially used to limit the interpolation matrix on each grid level to at most 3 coefficients per row, although c_{13} reaches around 16% of c_{12} . It thus appears that the strength-of-connection tolerance θ should be of the form

$$\theta = \frac{c_{13}}{c_{12}} + \epsilon_0, \tag{4.5}$$

where ϵ_0 is some small number, which can be chosen to be 10^{-5} in one-dimensional realistic problems.

As is known, Algorithm 4.1 is much more expensive for well-conditioned problems than basic iterative techniques, such as conjugate gradient (CG) or (plain) Jacobi iterative method. For the purpose of solving (2.6) in an optimal way, an adaptive AMG method is proposed below by combining Algorithm 4.1, the reference formula (4.5) and the condition number estimation (3.5) in Corollary 3.1 as the clear distinction to adaptively pick an appropriate solver.

Algorithm 4.2. An adaptive AMG method S_{ad} for the linear system (2.6).

Step 1 If the condition (3.5) is unsatisfied, then goto Step 2, else set S_{ad} as the CG or Jacobi iterative method;

Step 2 Set S_{ad} as the classical AMG method described in Algorithm 4.1, with θ chosen via the reference formula (4.5).

5 Performance evaluation

Let us illustrate the effectiveness of Algorithms 4.1 and 4.2. Numerical experiments are performed in a 64 bit Fedora 18 platform, double precision arithmetic on Intel Xeon (W5590) with 24.0 GB RAM, 3.33 GHz, with an -O2 optimization parameter. In the following tables, dashed entries (-) indicate the solutions either diverge or fail to converge after 1000 iterations, Its is the number of iterations until the stopping criterion 10^{-12} is reached, T_c represents the CPU time including both Setup and Solve phases with second as its unit, C_g and C_o respectively denote grid and operator complexities, which are defined as sums of the number of degrees of freedom and nonzero elements on all grid levels divided by those of the finest grid level, and used as measures for memory requirements, arithmetic operations and the execution time in Setup and Solve phases.

Example 5.1. Comparisons of the classical AMG over CG and Jacobi iterative methods for the case when (3.5) is satisfied with two different fractional orders.

Table 6: Number of iterations and wall time for the case $\tau=h^2$.

M	$\alpha = \beta = 0.6$						$\alpha = \beta = 0.8$					
	Jacobi		CG		AMG		Jacobi		CG		AMG	
	Its	T_c	Its	T_c	Its	T_c	Its	T_c	Its	T_c	Its	T_c
32	18	1.78E-4	9	1.09E-4	4	5.22E-4	22	2.03E-4	11	1.27E-4	5	2.84E-4
64	18	3.90E-4	11	2.19E-4	4	7.79E-4	23	4.84E-4	13	1.99E-4	5	6.33E-4
128	19	1.31E-3	11	4.60E-4	4	2.52E-3	23	1.54E-3	13	5.26E-4	5	1.89E-3
256	19	4.69E-3	11	1.57E-3	4	9.73E-3	23	5.66E-3	13	1.82E-3	5	7.06E-3
512	19	2.61E-2	11	8.03E-3	4	5.49E-2	23	3.12E-2	13	9.56E-3	5	4.57E-2
1024	19	1.95E-1	11	6.04E-2	4	1.73E-1	23	2.36E-1	12	6.53E-2	5	1.32E-1
2048	19	3.98E-1	11	1.22E-1	4	9.39E-1	23	9.11E-1	12	1.32E-1	5	7.49E-1
4096	19	3.03	11	9.25E-1	4	2.80	23	3.65	12	1.01	5	2.98

As expected, the results in Table 6 show that Jacobi, CG and AMG methods are robust with respect to the mesh size and fractional order, which indicates indirectly the correctness of (3.1). In addition, CG method runs 3.28 and 3.03 times faster than Jacobi and AMG methods for $M=4096$ and $\alpha = \beta = 0.6$, respectively.

Example 5.2. Comparisons between the classical AMG method and CG method for the case when (3.5) is unsatisfied.

As shown in Table 7, AMG method converges robustly regarding to the mesh size and may be weakly dependent of β , while the number of iterations of CG method is

Table 7: Number of iterations and wall time for the case $\tau=1/32$.

M	$\beta=0.6$				$\beta=0.8$				$\beta=0.99$			
	CG		AMG		CG		AMG		CG		AMG	
	<i>Its</i>	T_c	<i>Its</i>	T_c	<i>Its</i>	T_c	<i>Its</i>	T_c	<i>Its</i>	T_c	<i>Its</i>	T_c
512	97	0.119	8	0.042	180	0.209	8	0.069	256	0.314	3	0.032
1024	147	0.715	8	0.169	314	1.627	8	0.301	512	2.537	3	0.133
2048	223	2.230	8	0.677	546	6.037	8	0.772	>1000	-	3	0.532
4096	337	13.378	8	2.735	948	38.481	8	3.143	>1000	-	3	2.034

Table 8: Number of iterations and wall time for the case $\tau=h$.

M	$\alpha=0.2, \beta=0.6$				$\alpha=0.6, \beta=0.8$			
	CG		AMG		CG		AMG	
	<i>Its</i>	T_c	<i>Its</i>	T_c	<i>Its</i>	T_c	<i>Its</i>	T_c
128	40	1.686E-3	8	2.868E-3	57	2.310E-3	7	2.873E-3
256	62	9.090E-3	8	1.571E-2	99	1.622E-2	7	1.081E-2
512	95	1.523E-1	8	6.976E-2	171	2.626E-1	7	4.808E-2
1024	145	5.166E-1	8	2.916E-1	291	1.7895	7	2.063E-1

quite unstable and sometimes CG method even break down. Furthermore AMG method runs 12.24 times faster than CG method for $M=4096$ and $\beta=0.8$.

Table 8 shows the results of $\tau=h$. Despite the advantage in computational cost and robustness over CG method, AMG method is nearly independent of α and β in this circumstance. Meanwhile, by an investigation in terms of number of iterations in Tables 7 and 8, CG method converges faster because of the improvement in condition number from $\mathcal{O}(h^{-2\beta})$ to $\mathcal{O}(h^{\alpha-2\beta})$.

Example 5.3. Comparisons of S_{ad} over the classical AMG and CG methods when the i -th time step size τ_i is chosen to be

$$\tau_i = \begin{cases} h^2, & i=1, \dots, K_1, \\ 1/32, & i=K_1+1, \dots, K_1+K_2. \end{cases}$$

We can observe from Table 9 that S_{ad} and AMG methods are fairly robust as to the mesh size, roughly 10 and 6 on the average. Yet the average number of iterations of CG method varies from 85 to 142. Moreover S_{ad} has a considerable advantage over others in CPU time, runs 1.72 and 6.09 times faster than AMG and CG methods for $M=2048$ and $K_2=100$.

Example 5.4. Analyze effects of the strength-of-connection tolerance θ on the performance of the classical AMG method.

It is seen from Tables 10 and 11 that there is a unique threshold θ_0 independent of h which guarantees the robustness of the classical AMG method and makes number of

Table 9: Comparisons among S_{ad} , CG and AMG.

K_2	$M=1024, K_1=K_2$						$M=2048, K_1=K_2$					
	S_α		CG		AMG		S_α		CG		AMG	
	Its	T_c	Its	T_c	Its	T_c	Its	T_c	Its	T_c	Its	T_c
25	459	2.09	7994	9.99	303	2.91	458	8.65	13681	71.76	304	12.03
50	909	4.11	15900	19.65	603	5.79	895	17.25	27196	141.81	604	23.79
75	1337	6.54	23748	30.74	903	8.60	1320	25.59	40637	212.48	904	35.76
100	1760	8.54	31573	40.12	1201	11.92	1745	36.07	54038	292.03	1204	50.66

K_2	$M=1024, K_1=3K_2$						$M=2048, K_1=3K_2$					
	S_{ad}		CG		AMG		S_{ad}		CG		AMG	
	Its	T_c	Its	T_c	Its	T_c	Its	T_c	Its	T_c	Its	T_c
25	987	2.86	8522	11.10	553	5.42	970	11.87	14193	79.22	554	21.86
50	1912	5.81	16903	22.57	1088	10.52	1895	22.66	28196	158.78	1091	47.96
75	2837	8.05	25248	31.73	1563	15.23	2820	33.83	42137	230.60	1566	66.73
100	3760	10.82	33573	42.33	2036	20.03	3745	48.37	56038	294.82	2041	83.03

Table 10: Effect of θ on the classical AMG when $M=512$.

θ	$\beta=0.8$				$\beta=0.99$			
	Its	T_c	C_g	C_o	Its	T_c	C_g	C_o
0.0001	293	1.952	1.037	1.001	103	6.784E-1	1.170	1.021
0.001	83	5.618E-1	1.098	1.008	60	4.189E-1	1.498	1.124
0.00684	31	1.797E-1	1.202	1.029	32	1.374E-1	1.652	1.147
0.00685	31	1.789E-1	1.202	1.029	3	3.255E-1	1.975	1.331
0.01	23	1.020E-1	1.247	1.041	3	3.301E-2	1.975	1.331
0.1	13	6.209E-2	1.489	1.124	3	4.356E-2	1.975	1.331
0.16042	13	6.037E-2	1.489	1.124	3	4.118E-2	1.975	1.331
0.16043	7	4.699E-2	1.975	1.331	3	3.158E-2	1.975	1.331
0.25	7	4.736E-2	1.975	1.331	3	4.353E-2	1.975	1.331
0.5	7	4.710E-2	1.975	1.331	3	4.354E-2	1.975	1.331

Table 11: Effect of θ on the classical AMG when $M=2048$.

θ	$\beta=0.8$				$\beta=0.99$			
	Its	T_c	C_g	C_o	Its	T_c	C_g	C_o
0.0001	335	23.621	1.038	1.001	123	6.310	1.170	1.021
0.001	107	9.024	1.100	1.008	102	5.597	1.497	1.125
0.00684	33	3.096	1.207	1.029	33	2.055	1.662	1.148
0.00685	33	3.129	1.207	1.029	3	7.314E-1	1.993	1.333
0.01	26	2.551	1.249	1.042	3	5.369E-1	1.993	1.333
0.1	15	1.691	1.497	1.125	3	5.448E-1	1.993	1.333
0.1603	15	1.690	1.497	1.125	3	5.372E-1	1.993	1.333
0.1604	8	1.217	1.993	1.333	3	5.294E-1	1.993	1.333
0.2	8	1.219	1.993	1.333	3	5.294E-1	1.993	1.333
0.25	8	1.217	1.993	1.333	3	5.299E-1	1.993	1.333

iterations of the classical AMG monotonically decreasing when $\theta < \theta_0$, or even the classical AMG possibly diverge when θ is small enough, e.g., $\theta_0 = 0.16043$ and $\theta_0 = 0.00685$ for cases $\beta = 0.8$ and $\beta = 0.99$. By direct calculations, we have $c_{13}/c_{12} \approx 0.160426$ and $c_{13}/c_{12} \approx 0.006846$. Utilizing the relation (4.5) and $\epsilon_0 = 10^{-5}$, the corresponding values of θ are respectively larger than those of θ_0 . This confirms the reasonability of the reference formula (4.5).

6 Conclusions

In this paper, we propose the variational formulation for a class of time-space Caputo-Riesz fractional diffusion equations, prove that the resulting matrix is a symmetric Toeplitz matrix, an M-matrix by appending a very weak constraint and its condition number is bounded by $1 + \mathcal{O}(\tau^\alpha h^{-2\beta})$, introduce the classical AMG method and prove rigorously that its convergence rate is independent of time and space step sizes, provide explicitly a reference formula of the strength-of-connection tolerance to guarantee the robustness and predictable behavior of AMG method in all cases, and develop an adaptive AMG method via our condition number estimation to decrease the computation cost. Numerical results are all in conformity with the theoretical results and verify the reasonability of the reference formula and the considerable advantage of the proposed adaptive AMG algorithm over other traditional iterative methods, e.g., Jacobi, CG and the classical AMG methods.

Acknowledgements

This work is under auspices of National Natural Science Foundation of China (Nos. 11571293, 11601460, 11601462) and the General Project of Hunan Provincial Education Department of China (Nos. 16C1540, 17C1527). The authors would like to thank the editor and two anonymous reviewers for their constructive comments which helped us to improve the quality of the presentation.

References

- [1] F. LIU, P. ZHUANG, V. ANH, I. TURNER AND K. BURRAGE, *Stability and convergence of the difference methods for the space-time fractional advection-diffusion equation*, Appl. Math. Comput., 191(1) (2007), pp. 12–20.
- [2] Z. Q. DING, A. G. XIAO AND M. LI, *Weighted finite difference methods for a class of space fractional partial differential equations with variable coefficients*, J. Comput. Appl. Math., 233(8) (2010), pp. 1905–1914.
- [3] G. H. GAO AND Z. Z. SUN, *A compact finite difference scheme for the fractional sub-diffusion equations*, J. Comput. Phys., 230(3) (2011), pp. 586–595.
- [4] S. P. YANG, A. G. XIAO AND X. Y. PAN, *Dependence analysis of the solutions on the parameters of fractional delay differential equations*, Adv. Appl. Math. Mech., 3(5) (2011), pp. 586–597.

- [5] X. N. CAO, J. L. FU AND H. HUANG, *Numerical method for the time fractional Fokker-Planck equation*, Adv. Appl. Math. Mech., 4(6) (2012), pp. 848–863.
- [6] H. WANG AND T. S. BASU, *A fast finite difference method for two-dimensional space-fractional diffusion equations*, SIAM J. Sci. Comput., 34(5) (2012), pp. A2444–A2458.
- [7] D. L. WANG, A. G. XIAO AND H. L. LIU, *Dissipativity and stability analysis for fractional functional differential equations*, Fract. Calc. Appl. Anal., 18(6) (2015), pp. 1399–1422.
- [8] D. L. WANG, A. G. XIAO AND W. YANG, *Maximum-norm error analysis of a difference scheme for the space fractional CNLS*, Appl. Math. Comput., 257 (2015), pp. 241–251.
- [9] W. YANG, D. L. WANG AND L. YANG, *A stable numerical method for space fractional Landau-Lifshitz equations*, Appl. Math. Lett., 61 (2016), pp. 149–155.
- [10] L. B. FENG, P. ZHUANG, F. LIU, I. TURNER, V. ANH AND J. LI, *A fast second-order accurate method for a two-sided space-fractional diffusion equation with variable coefficients*, Comput. Math. Appl., 73(6) (2017), pp. 1155–1171.
- [11] D. D. HE AND K. J. PAN, *An unconditionally stable linearized difference scheme for the fractional Ginzburg-Landau equation*, Numer. Algor., (2018), doi: 10.1007/s11075-017-0466-y.
- [12] V. J. ERVIN AND J. P. ROOP, *Variational formulation for the stationary fractional advection dispersion equation*, Numer. Methods Partial Differ. Equ., 22(3) (2006), pp. 558–576.
- [13] H. ZHANG, F. LIU AND V. ANH, *Galerkin finite element approximation of symmetric space-fractional partial differential equations*, Appl. Math. Comput., 217(6) (2010), pp. 2534–2545.
- [14] K. BURRAGE, N. HALE AND D. KAY, *An efficient implicit FEM scheme for fractional-in-space reaction-diffusion equations*, SIAM J. Sci. Comput., 34(4) (2012), pp. A2145–A2172.
- [15] W. P. BU, Y. F. TANG AND J. Y. YANG, *Galerkin finite element method for two-dimensional Riesz space fractional diffusion equations*, J. Comput. Phys., 276 (2014), pp. 26–38.
- [16] K. MUSTAPHA, B. ABDALLAH AND K. M. FURATI, *A discontinuous Petrov-Galerkin method for time-fractional diffusion equations*, SIAM J. Numer. Anal., 52(5) (2014), pp. 2512–2529.
- [17] L. B. FENG, P. ZHUANG, F. LIU, I. TURNER AND Y. T. GU, *Finite element method for space-time fractional diffusion equation*, Numer. Algor., 72(3) (2016), pp. 749–767.
- [18] X. P. ZHANG, M. GUNZBURGER AND L. L. JU, *Quadrature rules for finite element approximations of 1D nonlocal problems*, J. Comput. Phys., 310 (2016), pp. 213–236.
- [19] W. P. BU, A. G. XIAO AND W. ZENG, *Finite difference/finite element methods for distributed-order time fractional diffusion equations*, J. Sci. Comput., 72(1) (2017), pp. 422–441.
- [20] Y. LIU, Z. D. YU, H. LI, F. LIU AND J. F. WANG, *Time two-mesh algorithm combined with finite element method for time fractional water wave model*, Int. J. Heat Mass Transfer, 120 (2018), pp. 1132–1145.
- [21] F. LIU, P. ZHUANG, I. TURNER, K. BURRAGE AND V. ANH, *A new fractional finite volume method for solving the fractional diffusion equation*, Appl. Math. Model., 38(15-16) (2014), pp. 3871–3878.
- [22] Y. M. LIN AND C. J. XU, *Finite difference/spectral approximations for the time-fractional diffusion equation*, J. Comput. Phys., 225(2) (2007), pp. 1533–1552.
- [23] Y. YANG, Y. P. CHEN AND Y. Q. HUANG, *Spectral-collocation method for fractional Fredholm integro-differential equations*, J. Korean Math. Soc., 51(1) (2014), pp. 203–224.
- [24] Y. YANG, Y. P. CHEN AND Y. Q. HUANG, *Convergence analysis of the Jacobi spectral-collocation method for fractional integro-differential equations*, Acta Math. Sci., 34B(3) (2014), pp. 673–690.
- [25] Y. YANG, *Jacobi spectral Galerkin methods for fractional integro-differential equations*, Calcolo, 52(4) (2015), pp. 519–542.
- [26] Y. YANG, *Jacobi spectral Galerkin methods for Volterra integral equations with weakly singular kernel*, Bull. Korean Math. Soc., 53(1) (2016), pp. 247–262.

- [27] S. P. YANG AND A. G. XIAO, *An efficient numerical method for fractional differential equations with two Caputo derivatives*, J. Comput. Math., 34(2) (2016), pp. 113–134.
- [28] T. MORONEY AND Q. Q. YANG, *A banded preconditioner for the two-sided, nonlinear space-fractional diffusion equation*, Comput. Math. Appl., 66(5) (2013), pp. 659–667.
- [29] J. H. JIA AND H. WANG, *Fast finite difference methods for space-fractional diffusion equations with fractional derivative boundary conditions*, J. Comput. Phys., 293 (2015), pp. 359–369.
- [30] X. M. GU, T. Z. HUANG, X. L. ZHAO, H. B. LI AND L. LI, *Strang-type preconditioners for solving fractional diffusion equations by boundary value methods*, J. Comput. Appl. Math., 277 (2015), pp. 73–86.
- [31] M. DONATELLI, M. MAZZA AND S. SERRA-CAPIZZANO, *Spectral analysis and structure preserving preconditioners for fractional diffusion equations*, J. Comput. Phys., 307 (2016), pp. 262–279.
- [32] H. K. PANG AND H. W. SUN, *Multigrid method for fractional diffusion equations*, J. Comput. Phys., 231 (2012), pp. 693–703.
- [33] W. P. BU, X. T. LIU, Y. F. TANG AND J. Y. YANG, *Finite element multigrid method for multi-term time fractional advection diffusion equations*, Int. J. Model. Simul. Sci. Comput., 6 (2015), 1540001.
- [34] Y. J. JIANG AND X. J. XU, *Multigrid methods for space fractional partial differential equations*, J. Comput. Phys., 302 (2015), pp. 374–392.
- [35] L. CHEN, R. H. NOCHETTO, E. OTÁROLA AND A. J. SALGADO, *Multilevel methods for nonuniformly elliptic operators and fractional diffusion*, Math. Comput., 85(302) (2016), pp. 2583–2607.
- [36] X. ZHAO, X. Z. HU, W. CAI AND G. E. KARNIADAKIS, *Adaptive finite element method for fractional differential equations using hierarchical matrices*, Comput. Methods Appl. Mech. Eng., 325 (2017), pp. 56–76.
- [37] M. H. CHEN AND W. H. DENG, *Convergence analysis of a multigrid method for a nonlocal model*, SIAM J. Matrix Anal. Appl., 38(3) (2017), pp. 869–890.
- [38] J. XU, *Iterative methods by space decomposition and subspace correction*, SIAM Rev., 34(4) (1992), pp. 581–613.
- [39] J. W. RUGE AND K. STÜBEN, *Algebraic multigrid*, in *multigrid methods*, Front. Appl. Math., 3 (1987), pp. 73–130.
- [40] J. XU AND L. ZIKATANOV, *Algebraic multigrid methods*, Acta Numer., 26 (2017), pp. 591–721.
- [41] K. STÜBEN, *An Introduction to Algebraic Multigrid*, in *Multigrid*, U. Trottenberg, C. W. Oosterlee and A. Schüller, eds., Academic Press, Singapore, 2001.